

Cardiac repair with intramyocardial injection of allogeneic mesenchymal stem cells after myocardial infarction

Luciano C. Amado^{*†}, Anastasios P. Saliaris^{*†}, Karl H. Schuleri^{*†}, Marcus St. John^{*}, Jin-Sheng Xie^{*}, Stephen Cattaneo[‡], Daniel J. Durand^{*†}, Torin Fitton[‡], Jin Qiang Kuang^{§¶}, Garrick Stewart^{*}, Stephanie Lehrke^{*†}, William W. Baumgartner[‡], Bradley J. Martin^{§¶}, Alan W. Heldman^{*†}, and Joshua M. Hare^{*†¶}

^{*}Department of Medicine, Cardiology Division, and [†]Department of Surgery, Division of Cardiac Surgery, The Johns Hopkins Hospital, Blalock 618, 600 North Wolfe Street, Baltimore, MD 21287; [‡]Institute for Cell Engineering, Broadway Research Building, Suite 651, 733 North Broadway, The Johns Hopkins University School of Medicine, Baltimore, MD 21205; and [§]Osiris Therapeutics, 2001 Aliceanna Street, Baltimore, MD 21231-3043

Communicated by Victor A. McKusick, The Johns Hopkins University School of Medicine, Baltimore, MD, June 2, 2005 (received for review April 13, 2005)

Although clinical trials of autologous whole bone marrow for cardiac repair demonstrate promising results, many practical and mechanistic issues regarding this therapy remain highly controversial. Here, we report the results of a randomized study of bone-marrow-derived mesenchymal stem cells, administered to pigs, which offer several new insights regarding cellular cardiomyoplasty. First, cells were safely injected by using a percutaneous-injection catheter 3 d after myocardial infarction. Second, cellular transplantation resulted in long-term engraftment, profound reduction in scar formation, and near-normalization of cardiac function. Third, transplanted cells were preprepared from an allogeneic donor and were not rejected, a major practical advance for widespread application of this therapy. Together, these findings demonstrate that the direct injection of cellular grafts into damaged myocardium is safe and effective in the periinfarct period. The direct delivery of cells to necrotic myocardium offers a valuable alternative to intracoronary cell injections, and the use of allogeneic mesenchymal stem cells provides a valuable strategy for cardiac regenerative therapy that avoids the need for preparing autologous cells from the recipient.

There is growing enthusiasm for the application of bone-marrow-derived cell-based therapies to repair or regenerate damaged myocardium. Small clinical trials conducted in the perimyocardial infarction (MI) period (1–5) with intracoronary infusion of autologous whole bone marrow preparations have suggested moderate improvements in cardiac function (1–3). However, recent experimental studies questioning the engraftment of hematopoietic stem cells (6, 7) and clinical findings that bone marrow cells do not engraft in the infarct zone or reduce infarct size have led to controversy regarding the mechanism behind these promising results (8).

Despite these concerns, there is increasing evidence that a specific bone marrow constituent, the mesenchymal stem cell (MSC), has cardiac reparative properties. MSCs engraft (9), have the potential for myocyte differentiation (10), and release cytokines and growth factors that stimulate endogenous repair mechanisms (11, 12). Furthermore, MSCs have several properties that contribute to an ability to evade rejection (13–15). In this regard, they lack cell-surface B-7 costimulatory molecules (16, 17) and may also directly inhibit inflammatory responses (18). Therefore, MSCs may serve as an allogeneic graft, thereby avoiding the need for bone marrow harvesting from prospective recipients, an extraordinary therapeutic advantage for this cell type.

An additional consideration for the development of cellular therapeutics is the delivery approach. As cited above, intracoronary infusions of cells do not appear to infiltrate the MI zone or reduce MI size (3). Accordingly, the direct delivery of cells into the area of tissue necrosis may circumvent this potential limitation of cellular delivery.

Here, to address the hypothesis that MSCs reduce MI size and improve cardiac function, we conducted a randomized, investigator-blinded, placebo-controlled trial of MSCs in pigs after MI. Additional studies were performed by using cardiac MRI. The aims of this study were to (i) demonstrate that stem cells can be safely administered directly to damaged myocardium via injection catheter, (ii) test the efficacy of preprepared allogeneic MSCs as a cardiac cellular therapeutic strategy, and (iii) test the prediction that the mechanism of benefit is cellular engraftment, which results in cardiac myocyte regeneration, reduced infarct size, and improved cardiac function.

Methods

Animal Model. All animal studies were approved by the Institutional Animal Care and Use Committee and comply with the *Guide for the Care and Use of Laboratory Animals* (National Institutes of Health Publication no. 80-23, revised 1985). Three different studies were conducted. First, we performed a randomized study of animals ($n = 14$) that underwent surgical induction of MI and instrumentation to measure left-ventricular (LV) performance and cardiac oxygen consumption. Second, a group of chronically instrumented animals ($n = 4$) were submitted to MI by balloon occlusion of the left anterior descending coronary artery (LAD), after recovery from surgery, so that measures of normal cardiac function could be obtained. Third, a group of animals ($n = 18$) were studied noninvasively with MRI after MI induced by balloon occlusion of the LAD.

Surgical Preparation. Female Yorkshire pigs underwent surgical instrumentation for subsequent noninvasive measurement of LV pressure and dimension and myocardial oxygen consumption (19, 20). The animals were instrumented, via a median sternotomy, with indwelling catheters in the descending aorta, right atrial appendage, and great cardiac vein. Endocardial ultrasound crystals (Sonometrics, Ontario, Canada) were inserted to measure short-axis dimension, and a pneumatic occluder was placed around the inferior vena cava for graded preload reduction to assess LV-pressure–dimension relations. A 4–5 mm flow probe (Transonics, Ithaca, NY) was placed around the mid-LAD to measure coronary volume flow. A solid-state miniature pressure transducer (P22, Konigsberg Instruments, Pasadena, CA) was placed in the LV apex for high-fidelity recordings of LV pressure. Additional pacing leads were

Abbreviations: Ees, ventricular elastance, slope of the end-systolic pressure–dimension relationship; LAD, left anterior descending coronary artery; LV, left ventricular; MI, myocardial infarction; MSC, mesenchymal stem cell; MVO₂, myocardial oxygen consumption per cardiac cycle; SW, stroke work.

[¶]J.Q.K. and B.J.M. are employees of Osiris Therapeutics.

^{||}To whom correspondence should be addressed. E-mail: jhare@mail.jhmi.edu.

© 2005 by The National Academy of Sciences of the USA

secured in the left atrial appendage for pacing during hemodynamic measurements.

During surgery, MI was induced by a 60-min occlusion of the LAD, followed by reperfusion. Stainless steel surgical clips were placed to delineate the injured myocardial area. At 3 d after MI, animals were randomized to receive intramyocardial injections of either allogeneic porcine MSCs (2.0×10^8 cells, $n = 7$) or placebo (Plasmalyte alone, Baxter Edwards Critical Care, Deerfield, IL; $n = 7$) under fluoroscopy, with a helical-needle-tipped injection catheter advanced to the left ventricle through a steerable guide catheter (BioCardia, South San Francisco, CA). MSC injections were guided by the presence and location of the surgical markers. Normal hemodynamic values in the swine were obtained from four additional animals after surgical preparation and instrumentation without coronary occlusion; two of these four were subjected to MI by a 1-h occlusion of the LAD with a balloon angioplasty catheter and received MSCs 3 d later, in a manner identical to that described above.

Hemodynamic and Energetic Measurements. Pressure–dimension data were recorded at steady state and during transient inferior vena cava occlusion. Myocardial contractility and/or work were indexed by the maximal rate of isovolumetric contraction ($+dP/dt$), stroke work (SW), and ventricular elastance, slope of the end-systolic pressure–dimension relationship (Ees) (21). Preload was analyzed as end-diastolic dimension and pressure, and afterload was evaluated as effective arterial elastance (22), the ratio of LV end-systolic pressure to stroke dimension. Diastolic function was indexed by LV end-diastolic pressure and the time constant of ventricular relaxation (τ ; Glantz formula) (23). Hemodynamic pressure–dimension data were digitized at 200 Hz and stored for subsequent analysis on a personal computer by using custom software. Myocardial oxygen consumption per cardiac cycle (MVO_2) was calculated from the arteriovenous difference of oxygen saturation in simultaneously sampled coronary sinus and aortic blood, multiplied by LAD flow and divided by heart rate. Cardiac mechanical efficiency was calculated as the SW/MVO_2 ratio (20).

MRI. To gain a better understanding of the effect of MSC therapy in the heart, infarct size and global function were assessed by MRI. MI was induced under fluoroscopic guidance: A catheter sheath (8 French) was placed in the right carotid artery, through which a coronary angioplasty balloon (3.5 French, 20 mm) was advanced into the proximal LAD. MI was created by inflating the balloon for 60 min, after which the balloon was deflated and the artery reperfused. After reperfusion, the catheter sheath in the carotid artery was removed, and the carotid artery was permanently closed. At 3 d after MI, animals were randomized to receive ($n = 6$) or not receive ($n = 6$) MSC therapy via catheter injection (Stiletto, Boston Scientific, Natick, MA). An additional group of animals ($n = 6$) received Feridex-labeled (Berlex Laboratories) MSCs, so as to visualize the cells by MRI. Cell retention was estimated by quantifying the presence and intensity of the hypoenhanced regions caused by the presence of iron-oxide-labeled cells.

MRI images were acquired by using a 1.5-T MR scanner (CV/i, GE Medical Systems, Waukesha, WI) at four time points after injection, 2 d and 1, 4, and 8 weeks. To assess engraftment of the MRI-labeled MSCs, high-resolution MRI images were obtained as described in ref. 24. Twelve to 18 contiguous short-axis images were acquired, covering the entire left ventricle, by using fast-gradient recoiled echo (24). Imaging parameters were as follows: repetition time (TR) = 8.7 ms; echo delay time (TE) = 2.4 ms, flip angle = 20° ; 512×512 matrix; 5-mm slice thickness/no gap; 32-kHz bandwidth; 28-cm FOV and 3 number of acquisitions (NSA).

Infarct size was analyzed by using the delayed-enhancement MRI (DE-MRI) technique (25). Images were acquired ≈ 15 min after the injection of contrast [Magnevist, Berlex Laboratories, gadolinium diethylenetriamine-pentaacetate dimeglumine (Gd-DTPA); 0.2

mmol/kg of body weight] by using an ECG-gated, breath-hold, interleaved, inversion recovery, fast-gradient recoiled echo pulse sequence. A total of 8–10 contiguous short-axis slices were prescribed to cover the entire left ventricle, from base to apex. Imaging parameters were as follows: TR/TE/inversion recovery time (TI) = 7.3 ms, 3.3 ms, and ≈ 200 ms; Flip angle = 25° ; 256×196 -160 matrix; 8-mm slice thickness/no gap; 31.2 kHz; 28-cm FOV and 2 NSA. Inversion recovery time was adjusted as needed to null the normal myocardium (25).

Global LV function was assessed by using a steady-state free-precession pulse sequence (26). Short-axis cine images were acquired at the same location as the DE-MRI images. Image parameters were as follows: TR/TE = 4.2 ms and 1.9 ms; flip angle = 45° ; 256×160 matrix; 8-mm slice thickness/no gap; 125 kHz; 28-cm FOV and 1 NSA. Images were analyzed by using a custom research software package (CINE TOOL, GE Medical Systems). Infarct areas were defined based on the full-width at half-maximum criterion (27).

Stem Cell Harvest and Isolation. Male swine MSCs were obtained, isolated, and expanded as described in ref. 9. Briefly, bone marrow was obtained from the iliac crest, and aspirates were passed through a density gradient to eliminate undesired cell types and were plated. At 5–7 d after plating, hematopoietic and other nonadherent cells were washed away during medium changes. The remaining purified MSC population was expanded in culture. All used cells were harvested when they reached 80–90% confluence at passage 3. MSCs were placed in a cryopreservation solution consisting of 10% DMSO, 5% porcine serum albumin, and 85% Plasmalyte. Cells were placed in cryo bags at a concentration of 5–10 million MSCs per ml and frozen in a control-rate freezer to -180°C until the day of implantation. By using trypan blue staining, the viability of all thawed MSC lots was verified to be $>85\%$ before use in the study. To ensure that the grafts were allogeneic, the MSC donor animals were of a different strain (Durok–Landrace) than the recipients (Yorkshire).

Cell Engraftment. Cell engraftment was assessed in the preparation of both surgical and nonsurgical (MRI) animals. First, in the surgically instrumented animals, MSCs were labeled after thawing with the cross-linkable membrane dye CM-DiI and the nuclear dye DAPI (Molecular Probes) according to the manufacturer's protocol, at a concentration of $2 \mu\text{g}/\text{ml}$ cell suspension. Before injection, the cells were thoroughly washed in serum-free DMEM, resuspended in 10 ml of PBS, and held on ice at an approximate concentration of 20 million cells per ml. Second, MRI studies were performed to demonstrate the location of intramyocardial cell delivery within the MI zone and to estimate the rate of cell engraftment throughout the 8-week study period. MSCs were magnetically labeled before injection by using a ferumoxide injectable solution (25 mg of Fe per ml, Feridex, Berlex Laboratories) (24). The presence of labeled MSCs within the myocardium was assessed by MRI at 2 d after injection and, subsequently, at 1, 4, and 8 weeks. Feridex labeling was also confirmed by Prussian blue stain immediately after injection.

Immunohistochemistry. The animals were followed for an 8-week period and were then humanely killed. Their hearts were analyzed at both microscopic and gross levels. Myocardial tissue was prepared for immunohistochemistry, as described in ref. 28. Tissue samples were obtained from three specific areas: infarct zone, infarct border zone, and remote tissue. Antibodies examined included α -actinin (Sigma), troponin-T (Sigma), tropomyosin (Sigma), myosin heavy chain-MHC (Developmental Studies Hybridoma Bank, University of Iowa, Iowa City), and phospholamban (Affinity BioReagents, Golden, CO). Ki67 and c-kit stains (Ventana Medical Systems, Tucson, AZ) were performed to assess the presence of active dividing and progenitor cells, respectively.

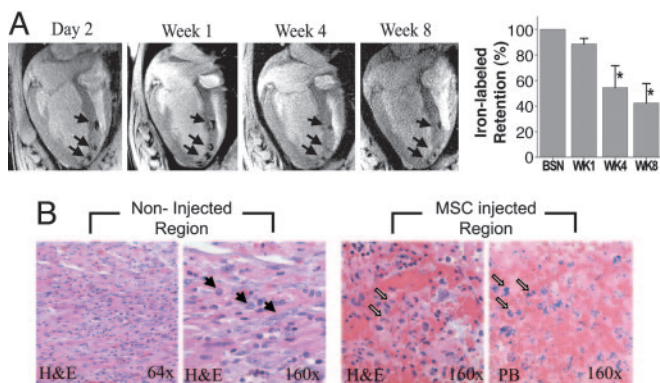


Fig. 1. Engraftment of allogeneic porcine MSCs assessed with MRI. (A) Pseudolong-axis image obtained after MSC injection. Magnetically labeled MSCs appear as hypoenhanced areas (arrows) visible at 2 d and at 1, 4, and 8 weeks after injection. (Right) Bar graph illustrating Feridex retention over 8 weeks. (B) Histologic evaluation of postinfarct myocardium. (Left) Hematoxylin/eosin (H&E) stains obtained from noninjected infarcted area, demonstrating an abundance of inflammatory cells (filled arrows) surrounding the necrotic region ($\times 160$ magnification). (Right) H&E and Prussian blue (PB) stains of MSC injection sites, demonstrating the absence of inflammatory cells. Open arrows indicate Feridex (iron)-labeled MSCs.

Infarct Size by Gross Pathology. Myocardial fibrosis was determined as a percentage of the left ventricle from whole-heart slices. For this purpose, hearts were excised and sectioned into 8-mm-thick short-axis slices. Each slice was weighed and digitally photographed. Analysis was performed in fresh, unstained hearts. TTC (2,3,5-triphenyltetrazolium chloride) staining was avoided, so as to preserve the myocardial tissue for engraftment-histological analysis. We have previously validated that quantification of infarct size is nearly identical between TTC-stained and unstained sections in the setting of chronic scarred tissue (data not shown). Infarcted areas and LV borders were manually traced for each slice by using a custom research software package IMAGE ANALYSIS 4.0.2 beta version (Scion, Frederick, MD). Infarct size was determined, in a blinded fashion, as percentage of LV mass from the digital pictures and normalized by the weight of the slice.

Statistical Analysis. All analyses were performed blind to the randomization. All values are expressed as mean \pm SEM. Hemodynamic parameters at baseline were compared between groups by using Student's *t* test. Differences in the hemodynamic indices during the 8-week period were compared within the groups by using repeated measurements ANOVA and between groups by using two-way ANOVA with an interaction term. A level of $P < 0.05$ was considered statistically significant.

Results

MSC Intramyocardial Injection. MSCs were injected via LV catheterization under fluoroscopic guidance in both surgically instrumented and MRI animals. The surgically instrumented animals ($n = 14$) were randomized to receive intramyocardial injections of either allogeneic porcine MSCs (13.7 ± 1 , ≈ 0.5 ml each) or placebo (13.4 ± 1 , ≈ 0.5 ml each). Additional animals ($n = 18$) underwent serial MRI imaging. At 3 d after MI, no animal had died, exhibited malignant arrhythmias, or demonstrated evidence of cardiac perforation during myocardial injections, thus demonstrating the safety of our delivery approach.

MSC Engraftment. Engraftment was monitored by both MRI and histological evaluation. MRI imaging of pigs receiving Feridex-labeled cells ($n = 6$) demonstrated a gradual loss of the intensity of the iron oxide label over the 2-month period, yet there was significant retention of implanted MSCs, with $42.4 \pm 15\%$ of the

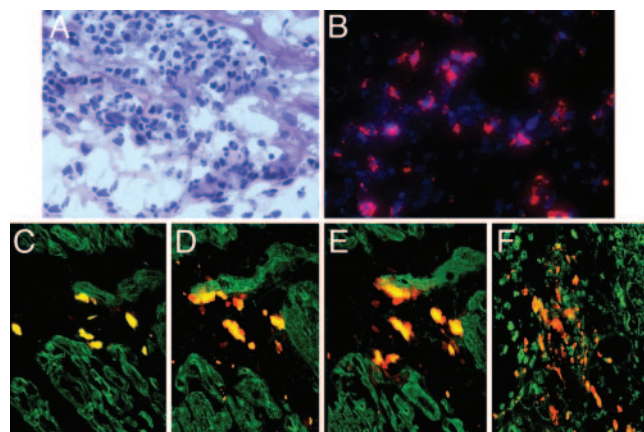


Fig. 2. Engraftment and differentiation of MSCs. DAPI- and Di-I-labeled MSCs (blue-staining nuclei and red-staining membranes, respectively) and fluorescent muscle-protein-specific antibodies (green). (A) Hematoxylin/eosin (H&E)-stained section and corresponding fluorescent detection of cellular labels. (B) A cluster of MSCs in proximity to host myocardium. Several muscle-specific proteins are detected by immunofluorescence, including α -actinin (C), phospholamban (D), tropomyosin (E), and troponin T (F). Yellow fluorescence indicates colocalization of immunofluorescent antibodies and DiI.

magnetic label detected at the end of 8 weeks (Fig. 1; $P < 0.05$ vs. 2 d postinjection). Histologic evaluation of the infarct, border zone, and remote myocardium was performed in the surgically instrumented animals that received Di-I- and DAPI-labeled cells. MSCs labeled with these membrane and nuclear dyes, respectively, ($n = 7$) were present throughout the infarct regions and border zones up to 8 weeks after implantation and expressed muscle-specific proteins not expressed by cultured MSCs (Fig. 2). MSCs were also detected in vascular structures, where they expressed vascular endothelium growth factor and Von Willebrand factor, suggesting differentiation and/or incorporation into vascular smooth muscle and/or endothelium (data not shown). Extracardiac MSC engraftment, differentiation into ectopic tissues (adipose, bone, cartilage, and tendon), and cardiac inflammatory infiltrates were not detected (Fig. 1B).

Impact of MSC Treatment on Infarct Size. Gross pathologic examination revealed that MSC treatment substantially decreased the percentage of left ventricle occupied by fibrosis (Fig. 3A). In the surgical group, placebo pigs exhibited scar tissue occupying $16 \pm 4.6\%$ of the left ventricle, and infarcts were transmural, beginning subendocardially and extending $>50\%$ of the LV-wall thickness, a finding similar to that observed in humans surviving MI with reperfusion of infarct-related arteries (29). However, in MSC-treated pigs, only $3.4 \pm 1.2\%$ of the left ventricle was occupied by scar tissue ($P = 0.008$ vs. placebo, Fig. 3A and B). Interestingly, in the MSC-treated group, the infarct region was confined to the midmyocardium, and viable tissue was clearly visible at both the subendocardial and subepicardial zones (Fig. 3C and D). The subendocardial tissue rim is consistent with the growth of new tissue, because myocardial infarction is known to develop in a wave-front pattern, progressing from the subendocardium toward the subepicardial layer (30). We further substantiated this observation in the MRI animals, where we measured the thickness of this rim on gross pathology in treated vs. control animals. Indeed, the rim was substantially thicker in MSC-treated vs. nontreated animals (2.4 ± 0.2 and 1.5 ± 0.2 mm, respectively; $n = 6$ each, Fig. 3E, $P < 0.05$).

To delineate mechanisms for the growth of this tissue rim, we evaluated MSC-injected tissue 10 d after cell injection. Immunohistochemical analysis of MI and MI border zones in MSC-treated animals revealed the presence of a band of myocytes positive for

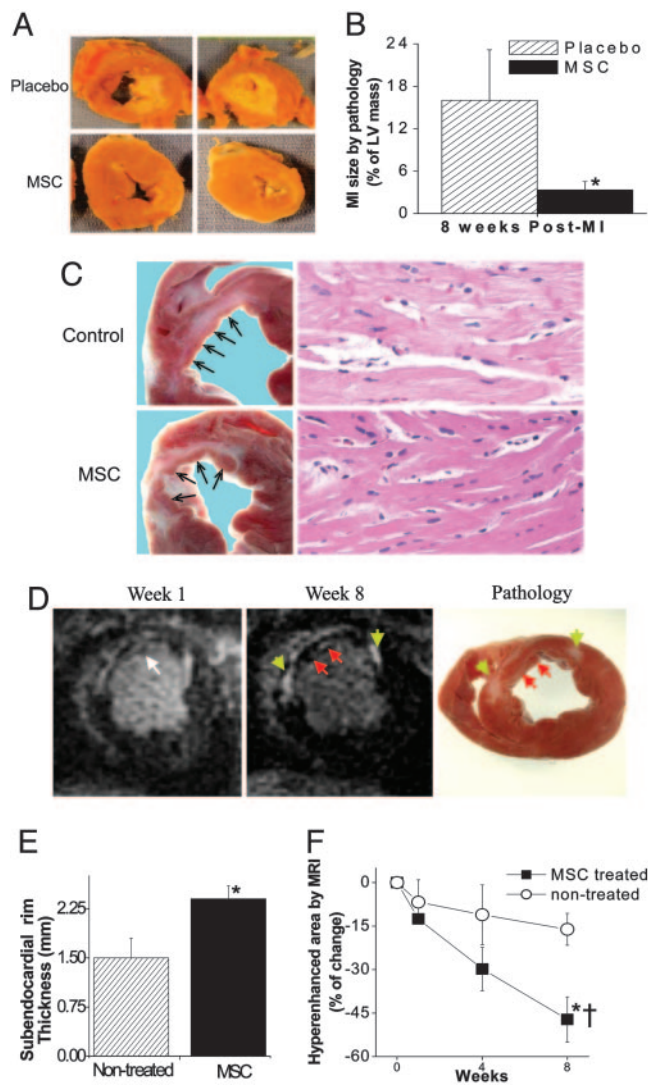


Fig. 3. Impact of MSC injection on myocardial morphology. (A) Representative example of MI scar formation in placebo-treated (Upper) and MSC-treated (Lower) animals at 8 weeks after injury. MSC injection reduces the scar, which is confined to the midmyocardium because of viable tissue in subendocardial and subepicardial zones. (B) Bar graph depicting MI size as the percentage of LV mass in MSC-treated vs. placebo-treated pigs in a randomized study (*, $P = 0.008$). (C) MSC cardiomyoplasty augments development of new myocardium (Left). At 8 weeks after MI, the subendocardial rim is thicker in the MSC group (arrows). Hematoxylin/eosin (H&E) stain of the subendocardial rim demonstrates cardiomyocytes in both control and MSC ($\times 100$ magnification). (D) Short-axis delayed-enhancement images, illustrating the change in infarct size after MSC treatment. At 1 week after MSC injection, there is anteroseptal myocardial necrosis and extensive microvascular obstruction (white arrow in Left). MSC administration leads to myocardial tissue regeneration (red arrows) and reduction of necrotic myocardium (yellow arrows) 8 weeks later (Center). (Left) Corresponding gross pathology. (E) Bar graph, depicting enhanced thickness of subendocardial viable tissue with MSCs (*, $P < 0.05$ vs. nontreated) after 8 weeks. (F) MI size assessed from MRI delayed hyperenhancement, showing that, in nontreated animals, infarct size does not decrease but is reduced $\approx 50\%$ with MSC treatment (*, $P < 0.05$ vs. baseline images obtained 2 d after therapy; †, $P < 0.05$ vs. nontreated).

c-kit- and Ki-67-staining cells 10 d after MI (Fig. 4). This band was not present in control animals, although both groups contained c-kit-positive hematopoietic cells in capillaries. This finding is consistent with both MSC differentiation and a paracrine effect, stimulating endogenous cellular replication, both of which are implicated as mechanisms for cardiac regenerative therapy (31, 32).

We next determined the time course of infarct size reduction with

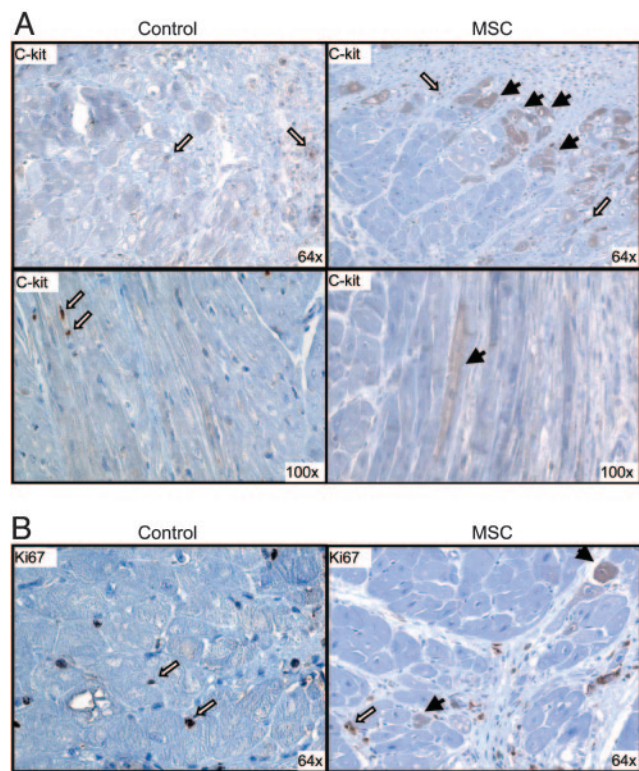


Fig. 4. Myocardial regeneration in MSC-treated hearts. Immunohistochemical evaluation of the subendocardial rim of infarcted myocardium 10 d postinjection. (A) Rim of c-Kit-positive myocytes (filled arrow) is visible along the infarct border in both groups and within capillaries (open arrow) in MSC but not in control group. (B) Ki67-positive myocytes present within MSC-treated heart.

MRI. Delayed-enhancement MRI confirmed the decrease in MI size observed at the time of postmortem analysis. MSC treatment significantly reduced the extent of necrotic myocardium throughout the course of the study (from 20.7 ± 3.5 to $9.9 \pm 1.3\%$ of the left ventricle, at 3 d and at 8 weeks, respectively; $P < 0.05$, $n = 6$), whereas infarct size did not decrease in control animals ($n = 6$) (Fig. 2F, $P < 0.05$ vs. MSC group).

MSC Therapy Effect on Cardiac Function. We next examined whether this new tissue formation translated into functional recovery and measured the effect of MSC therapy on post-MI hemodynamics in animals ($n = 14$) instrumented as described in refs. 19 and 20. Table 1 depicts indices of ventricular function before MI creation and at 3 d after MI in the two treatment groups (MSC or placebo injections). As shown, there is a sizable and nearly identical reduction in systolic (decreased peak $+dP/dt$ and Ees) and diastolic function (increased LVPED and τ) ($P < 0.05$ vs. normal pre-MI values), in both groups, indicative of equivalent degrees of injury.

In the placebo-treated group ($n = 7$), impaired cardiac function evident at 3 d after MI showed either no sign of recovery or a tendency to worsen over 8 weeks of follow-up: Indices of myocardial contraction fell, and end-diastolic pressure rose, as did τ (Table 1 and Fig. 5). In marked contrast, animals receiving MSCs ($n = 7$) exhibited recovery to essentially normal levels of both systolic [Ees rose to 17.1 ± 2 mmHg/mm (1 mmHg = 133 Pa) and peak $+dP/dt$ to $2,465 \pm 574$ mmHg/sec; Fig. 5 and Table 1] and diastolic function (τ fell to 34.2 ± 1.2 msec; Fig. 5). LV end-diastolic pressure did not return to normal levels at 8 weeks, although a significant improvement was observed ($P < 0.05$ vs. placebo group; Table 1).

To further evaluate the effect of MSC therapy on global cardiac function, MRI determination of LV ejection fraction (LVEF) was performed. Immediately after MI, there was a marked deteriora-

Table 1. Hemodynamic measurements

	Normal	3 d post-MI		8 weeks post-MI	
		Placebo	MSC	Placebo	MSC
LV end-diastolic pressure, mm Hg	8.4 ± 2.3	21.5 ± 5.8*	26 ± 3.6*	29.8 ± 7.6	20 ± 6.4†
LV end-systolic pressure, mm Hg	107.1 ± 4.2	98.8 ± 6.6	112.6 ± 5.6	117.7 ± 22.2	113.8 ± 5.8
Arterial elastance, mm Hg/mm	14 ± 2	20 ± 2.5	24.8 ± 4.2	26.1 ± 8.7	17.1 ± 3
dP/dt _{max} , mm Hg/s	2,560 ± 266	1,734 ± 218*	1,802 ± 80*	1,720 ± 351	2,465 ± 574†
Ees, mm Hg/mm	16.3 ± 2.4	11.2 ± 0.5*	8.1 ± 3.1*	7.9 ± 1.2	17.1 ± 2†
τ, ms	36.2 ± 1.8	42 ± 1*	44.3 ± 2.3*	52.6 ± 11.6	34.2 ± 1.2†
SW, mm Hg/mm	771 ± 116.5	434.8 ± 59.9*	374.4 ± 59.3*	470.3 ± 86.9	654.4 ± 129.3†
MVO ₂ , J per beat	3.2 ± 0.9	7.4 ± 1.4*	10.3 ± 2*	12.9 ± 1.4†	3.7 ± 1.8†
SW/MVO ₂	9.1 ± 1.6	3.8 ± 0.8*	2.5 ± 0.6*	2.9 ± 0.1†	10 ± 5.6†

MVO₂ indicates myocardial oxygen consumption and SW/MVO₂ myocardial efficiency.

**P* < 0.05 vs. normal (pre-MI).

†*P* < 0.05 vs. placebo (2-way ANOVA).

‡Listed values were measured at 4 weeks.

tion in LVEF, (25.3 ± 1.6 and $29.8 \pm 1.9\%$ for MSC- and nontreated animals, respectively, $P = \text{NS}$). However, whereas there was minimal change in LVEF in the nontreated group ($n = 6$), LVEF increased from 25.3 ± 1.6 to $41.9 \pm 0.7\%$ in MSC-treated animals ($P < 0.05$ vs. nontreated, $n = 6$; see supporting information, which is published on the PNAS web site) during the 8-week follow-up period.

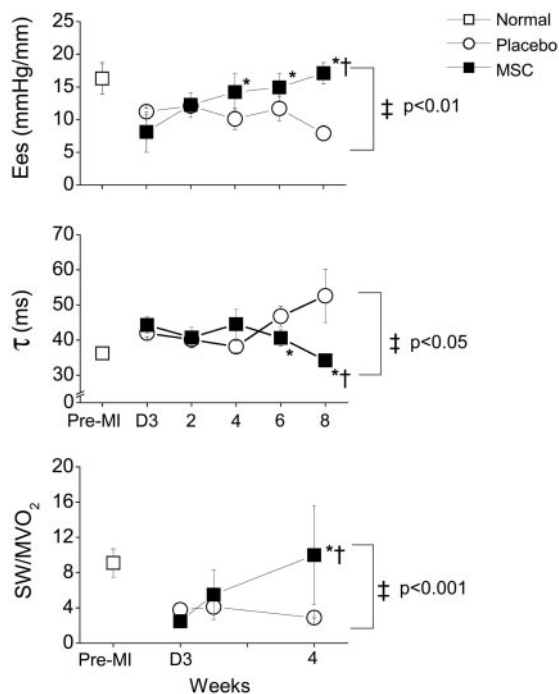


Fig. 5. Physiologic impact of MSC therapy after MI. Immediately after MI (D3, day 3), systolic and diastolic cardiac functions are impaired in both groups ($P = \text{NS}$ for differences between groups at day 3 after MI). (Top) Ventricular elastance (Ees) declines in placebo-treated pigs but increases dramatically in the MSC group, with complete restoration of Ees to normal levels at 8 weeks ($P = \text{NS}$ vs. normal). (Middle) Isovolemic ventricular relaxation (τ) returns to normal in MSC-treated pigs but remains impaired in placebo-treated pigs. (Bottom) The impact of MSC therapy on myocardial mechanoenergetics (SW/MVO₂) precedes the restoration of systolic and diastolic cardiac function. During the 4 weeks after MI, SW declines in placebo-treated animals, whereas MVO₂ increases, leading to a reduced SW/MVO₂ ratio. In MSC-treated pigs, SW increases and MVO₂ decreases, resulting in augmented SW/MVO₂ and restoration of mechanoenergetic coupling toward normal [$P < 0.05$ vs. D3, respectively, by repeated measurements ANOVA (†); *, $P < 0.05$ by Bonferroni; ‡, $P < 0.05$ between groups by two-way ANOVA].

Post-MI heart failure is characterized by mechanoenergetic uncoupling, a phenomenon in which MVO₂ increases, despite decreased cardiac work (33, 34). In both groups, cardiac energy metabolism was impaired after MI ($P < 0.05$ vs. normal pre-MI values; Table 1 and Fig. 5). In placebo-treated animals, SW decreased substantially during 4 weeks, accompanied by a paradoxical gain in MVO₂ (Table 1), both factors together depressing the SW/MVO₂ ratio (Fig. 5). Conversely, MSC therapy significantly improved myocardial efficiency, increasing SW (from 374.4 ± 59.3 to 654.4 ± 129.3 mmHg/mm at 8 weeks; Table 1), while simultaneously decreasing MVO₂ (from 10.3 ± 2 to 3.7 ± 1.8 J per beat), both toward normal (Table 1). Thus, MSC therapy exerts favorable effects on the damaged heart that extends to improved energy metabolism. The SW/MVO₂ ratio increased from 2.5 ± 0.6 at 3 d after MI to a normal level of 10 ± 5.6 ($P < 0.05$ vs. placebo; Fig. 5) at 4 weeks. The restoration in mechanoenergetics was the earliest observable benefit of MSC treatment, preceding the changes in global cardiac function.

Discussion

The present work addresses major issues regarding cardiac regenerative therapy. Here, we show that, in pigs, allogeneic MSCs can be safely and effectively delivered via injection catheter to a region of damaged myocardium, where they engraft and express proteins normally restricted to cardiac myocytes, vascular endothelium, and smooth muscle. Engrafted MSCs dramatically reduce the extent of necrotic myocardium and promote the regeneration of new, contractile myocardium along the subendocardial surface of the MI. These effects produce early recovery of cardiac energy metabolism, followed by near-normalization of systolic and diastolic cardiac function and substantial increases in global cardiac performance. Taken together, these findings offer therapeutic promise for the application of cellular therapeutics to myocardial infarction. Importantly MSCs have the potential to be administered as a preprepared allogeneic graft, avoiding the need to perform bone marrow harvests on recipient patients.

Both experimental (6, 35) and clinical (1, 3) studies have contributed to the controversy surrounding the extent and mechanism of cardiac repair resulting from bone marrow cellular therapy. In experiments conducted on mice, bone marrow c-kit-positive cells have the capacity to engraft in damaged myocardium and differentiate into cardiac myocytes (35, 36). On the other hand, several reports have demonstrated that CD34⁺ hematopoietic stem cells do neither (6, 7). Several small clinical trials demonstrate that autologous whole bone marrow infused into the coronary artery marginally improves the ejection fraction (3). Importantly, whole bone marrow cells are reported by positron emission tomography scanning to be unable to infiltrate areas of myocyte necrosis (8).

Based on concerns regarding the ability of bone marrow preparations to enter the region of damaged myocardium (8), we predicted that direct injection would enhance cell engraftment. Indeed, catheter-based cell injection was safe and highly effective, producing areas of regenerated myocardium and diminishing the amount of fibrotic tissue. Functionally, this therapy essentially normalized systolic and diastolic cardiac function. This approach represents a potential advance over the majority of clinical trials, which have used intracoronary techniques for cell delivery, have shown only minimal improvement in cardiac function, and have had variable success in reducing infarct size (1–4, 37). The relative contribution to the degree of recovery we report here of cell type vs. the delivery method remains unclear. It should be mentioned that previous reports suggest that intracoronary infusion of MSCs may not be feasible, given the size of these cells and their propensity to cause microvascular obstruction (38). On the other hand, there is a possibility that intravenously administered MSCs may track to the heart in response to injury signals (39).

This study demonstrates the potential therapeutic effects of allogeneic MSC transplantation after MI. MSCs are easily obtained from bone marrow and, because of their multilineage potential (9, 10) and immunological advantages (16–18), represent ideal candidates for allogeneic cell therapy. Our findings are supported by earlier studies in rats, in which MSCs, genetically modified to survive in ischemic myocardium, decreased infarct size (40). The present results indicate that unmodified allogeneic cells are therapeutically useful and, therefore, offer substantial practical advances for the application of this therapy. Indeed, clinical trials for allogeneic MSC therapy have received FDA approval.

The mechanism by which cellular therapy limits the extent of damaged myocardium after ischemic insult remains highly controversial, and three general mechanisms are proposed: transdifferentiation (35, 40), cell fusion (41), and paracrine signaling (42). It

may be argued, however, that the net result of effective cellular therapy is a reduction in size of the MI and restoration of myocardial contraction. Here, we describe evidence of cardiac myocyte regeneration. Our results are consistent with the presence of both mechanisms, transdifferentiation of transplanted MSCs into the cardiac myocyte lineage and increased endogenous repair mechanisms (31). There is growing awareness that both cell differentiation and paracrine effects are operative in cellular regenerative strategies (31, 43). Indeed, the presence of endogenous cardiac stem cells provides a plausible target for paracrine signaling due to injected MSCs (44–47). Our findings that MSCs express VEGF, which is linked to both neoangiogenesis (48) and stem cell homing and migration (11, 49), also support a contribution of paracrine stimulation of endogenous repair mechanisms.

Proarrhythmia is a major concern surrounding the use of cellular cardiomyoplasty. We did not observe this complication, rather, noting a trend toward decreased sudden death in MSC-treated animals (L.C.A. and J.M.H., unpublished observations), suggesting that the implantation of MSCs into infarcted myocardium is safe and, perhaps, even protects from postinfarct arrhythmias.

In summary, allogeneic MSCs injected into regions of damaged myocardium 3 d after MI engraft, stimulate cardiac regeneration, and profoundly decrease myocardial infarct size. As a result, there is an early restoration of cardiac energy metabolism, followed by dramatic improvements in ejection fraction and near-normalization in both systolic and diastolic cardiac function. The successful application of allogeneic cells injected intramyocardially offers insights for practical application of this therapy in future clinical study.

This work was supported by The Johns Hopkins University School of Medicine Institute for Cell Engineering, Osiris Therapeutics, The Donald W. Reynolds Foundation, and National Institutes of Health Grants R21 HL-72185 and R01 NIA AG025017.

- Schachinger, V., Assmus, B., Britten, M. B., Honold, J., Lehmann, R., Teupe, C., Abolmaali, N. D., Vogl, T. J., Hofmann, W. K., Martin, H., et al. (2004) *J. Am. Coll. Cardiol.* **44**, 1690–1699.
- Britten, M. B., Abolmaali, N. D., Assmus, B., Lehmann, R., Honold, J., Schmitt, J., Vogl, T. J., Martin, H., Schachinger, V., Dimmeler, S., et al. (2003) *Circulation* **108**, 2212–2218.
- Wollert, K. C., Meyer, G. P., Lotz, J., Ringes-Lichtenberg, S., Lippolt, P., Breidenbach, C., Fichtner, S., Korte, T., Hornig, B., Messinger, D., et al. (2004) *Lancet* **364**, 141–148.
- Assmus, B., Schachinger, V., Teupe, C., Britten, M., Lehmann, R., Dohert, N., Grunwald, F., Aicher, A., Urbich, C., Martin, H., et al. (2002) *Circulation* **106**, 3009–3017.
- Strauer, B. E., Brehm, M., Zeus, T., Kosterling, M., Hernandez, A., Sorg, R. V., Kogler, G., & Wernet, P. (2002) *Circulation* **106**, 1913–1918.
- Murry, C. E., Soonpaa, M. H., Reinecke, H., Nakajima, H., Nakajima, H. O., Rubart, M., Pasumarthi, K. B., Ismail, V. J., Bartelmez, S. H., Poppa, V., et al. (2004) *Nature* **428**, 664–668.
- Balsam, L. B., Wagers, A. J., Christensen, J. L., Kofidis, T., Weissman, I. L., & Robbins, R. C. (2004) *Nature* **428**, 668–673.
- Hofmann, M., Wollert, K. C., Meyer, G. P., Menke, A., Arseniev, L., Hertenstein, B., Ganser, A., Knapp, W. H., & Drexler, H. (2005) *Circulation* **111**, 2198–2202.
- Pittenger, M. F., Mackay, A. M., Beck, S. C., Jaiswal, R. K., Douglas, R., Mosca, J. D., Moorman, M. A., Simonetti, D. W., Craig, S., & Marshak, D. R. (1999) *Science* **284**, 143–147.
- Makino, S., Fukuda, K., Miyoshi, S., Konishi, F., Kodama, H., Pan, J., Sano, M., Takahashi, T., Hori, S., Abe, H., et al. (1999) *J. Clin. Invest.* **103**, 697–705.
- Tang, Y. L., Zhao, Q., Zhang, Y. C., Cheng, L., Liu, M., Shi, J., Yang, Y. Z., Pan, C., Ge, J., & Phillips, M. I. (2004) *Regul. Pept.* **117**, 3–10.
- Kucia, M., Dawn, B., Hunt, G., Guo, Y., Wysoczynski, M., Majka, M., Ratajczak, J., Rezzoug, F., Ildstad, S. T., Bollen, R., et al. (2004) *Circ. Res.* **95**, 1191–1199.
- Bartholomew, A., Sturgeon, C., Siatskas, M., Ferrer, K., McIntosh, K., Patil, S., Hardy, W., Devine, S., Ucker, D., Deans, R., et al. (2002) *Exp. Hematol.* **30**, 42–48.
- Le Blanc, K., Tammik, L., Sundberg, B., Haynesworth, S. E., & Ringden, O. (2003) *Scand. J. Immunol.* **57**, 11–20.
- Tse, W. T., Pendleton, J. D., Beyer, W. M., Egalka, M. C., & Guinan, E. C. (2003) *Transplantation* **75**, 389–397.
- Majumdar, M. K., Keane-Moore, M., Buyaner, D., Hardy, W. B., Moorman, M. A., McIntosh, K. R., & Mosca, J. D. (2003) *J. Biomed. Sci.* **10**, 228–241.
- Le Blanc, K., Tammik, C., Rosendahl, K., Zetterberg, E., & Ringden, O. (2003) *Exp. Hematol.* **31**, 890–896.
- Di Nicola, M., Carlo-Stella, C., Magni, M., Milanese, M., Longoni, P. D., Matteucci, P., Grisanti, S., & Gianni, A. M. (2002) *Blood* **99**, 3838–3843.
- Saavedra, W. F., Paolucci, N., St. John, M. E., Skaf, M. W., Stewart, G. C., Xie, J. S., Harrison, R. W., Zeichner, J., Mudrick, D., Marban, E., et al. (2002) *Circ. Res.* **90**, 297–304.
- Ekelund, U. E., Harrison, R. W., Shoket, O., Thakkar, R. N., Tunin, R. S., Senzaki, H., Kass, D. A., Marban, E., & Hare, J. M. (1999) *Circ. Res.* **85**, 437–445.
- Hare, J. M., Kass, D. A., & Stamler, J. S. (1999) *Nat. Med.* **5**, 1241–1242.
- Kelly, R. P., Ting, C.-T., Yang, T.-M., Liu, C.-P., Maughan, W. L., Chang, M.-S., & Kass, D. A. (1992) *Circulation* **86**, 513–521.
- Gilbert, J. C., & Glantz, S. A. (1989) *Circ. Res.* **64**, 827–852.
- Kraichman, D. L., Heldman, A. W., Atalar, E., Amado, L. C., Martin, B. J., Pittenger, M. F., Hare, J. M., & Bulte, J. W. (2003) *Circulation* **107**, 2290–2293.
- Simonetti, O. P., Kim, R. J., Fieno, D. S., Hillenbrand, H. B., Wu, E., Bundy, J. M., Finn, J. P., & Judd, R. M. (2001) *Radiology* **218**, 215–223.
- Slavin, G. S., & Saranathan, M. (2002) *Magn. Reson. Med.* **48**, 934–941.
- Amado, L. C., Gerber, B. L., Gupta, S. N., Rettmann, D. W., Szarf, G., Schock, R., Nasir, K., Kraitchman, D. L., & Lima, J. A. (2004) *J. Am. Coll. Cardiol.* **44**, 2383–2389.
- Shake, J. G., Gruber, P. J., Baumgartner, W. A., Senechal, G., Meyers, J., Redmond, J. M., Pittenger, M. F., & Martin, B. J. (2002) *Ann. Thorac. Surg.* **73**, 1919–1925.
- Christian, T. F., Schwartz, R. S., & Gibbons, R. J. (1992) *Circulation* **86**, 81–90.
- Garcia-Dorado, D., Theroux, P., Desco, M., Solares, J., Elizaga, J., Fernandez-Aviles, F., Alonso, J., & Soriano, J. (1989) *Am. J. Physiol.* **256**, H1266–H1273.
- Dimmeler, S., Zeiher, A. M., & Schneider, M. D. (2005) *J. Clin. Invest.* **115**, 572–583.
- Pittenger, M. F., & Martin, B. J. (2004) *Circ. Res.* **95**, 9–20.
- Trines, S. A., Slager, C. J., Onderwater, T. A., Lamers, J. M., Verdouw, P. D., & Krams, R. (2001) *Cardiovasc. Res.* **51**, 122–130.
- Hayashi, Y., Takeuchi, M., Takaoka, H., Hata, K., Mori, M., & Yokoyama, M. (1996) *Circulation* **93**, 932–939.
- Kajstura, J., Rota, M., Whang, B., Cascapera, S., Hosoda, T., Bearzi, C., Nurzynska, D., Kasahara, H., Zias, E., Bonafe, M., et al. (2004) *Circ. Res.* **96**, 127–137.
- Orlic, D., Kajstura, J., Chimenti, S., Jakoniuk, I., Anderson, S. M., Li, B., Pickel, J., McKay, R., Nadal-Ginard, B., Bodine, D. M., et al. (2001) *Nature* **410**, 701–705.
- Ziegelhoeffer, T., Fernandez, B., Kostin, S., Heil, M., Voswinckel, R., Helisch, A., & Schaper, W. (2004) *Circ. Res.* **94**, 230–238.
- Vulliet, P. R., Greeley, M., Halloran, S. M., MacDonald, K. A., & Kittleson, M. D. (2004) *Lancet* **363**, 783–784.
- Nagaya, N., Fujii, T., Iwase, T., Ohgushi, H., Itoh, T., Uematsu, M., Yamagishi, M., Mori, H., Kangawa, K., & Kitamura, S. (2004) *Am. J. Physiol.* **287**, H2670–H2676.
- Mangi, A. A., Noisieux, N., Kong, D., He, H., Rezvani, M., Ingwall, J. S., & Dzau, V. J. (2003) *Nat. Med.* **9**, 1195–1201.
- Nygren, J. M., Jovinge, S., Breitbach, M., Sawen, P., Roll, W., Hescheler, J., Taneera, J., Fleischmann, B. K., & Jacobsen, S. E. (2004) *Nat. Med.* **10**, 494–501.
- Fraidenraich, D., Stillwell, E., Romero, E., Wilkes, D., Manova, K., Basson, C. T., & Benezra, R. (2004) *Science* **306**, 247–252.
- Yoon, Y. S., Wecker, A., Heyd, L., Park, J. S., Tkebuchava, T., Kusano, K., Hanley, A., Scadova, H., Qin, G., Cha, D. H., et al. (2005) *J. Clin. Invest.* **115**, 326–338.
- Beltrami, A. P., Barlucchi, L., Torella, D., Baker, M., Limana, F., Chimenti, S., Kasahara, H., Rota, M., Musso, E., Urbaneck, K., et al. (2003) *Cell* **114**, 763–776.
- Oh, H., Bradfute, S. B., Gallardo, T. D., Nakamura, T., Gaussin, V., Mishina, Y., Pocius, J., Michael, L. H., Behringer, R. R., Garry, D. J., et al. (2003) *Proc. Natl. Acad. Sci. USA* **100**, 12313–12318.
- Laugwitz, K. L., Moretta, A., Lam, J., Gruber, P., Chen, Y., Woodard, S., Lin, L. Z., Cai, C. L., Lu, M. M., Reth, M., et al. (2005) *Nature* **433**, 647–653.
- Messina, E., De Angelis, L., Frati, G., Morrone, S., Chimenti, S., Fiordaliso, F., Salio, M., Battaglia, M., Latronico, M. V., Coletta, M., et al. (2004) *Circ. Res.* **95**, 911–921.
- Kocher, A. A., Schuster, M. D., Szabolcs, M. J., Takuma, S., Burkoff, D., Wang, J., Homma, S., Edwards, N. M., & Itescu, S. (2001) *Nat. Med.* **7**, 430–436.
- Eriksson, U., & Alitalo, K. (2002) *Nat. Med.* **8**, 775–777.